

Article

Relative Availability of Nitrogen and Calcium Regulates the Growth of Poplar Seedlings Due to Transcriptome Changes

Xiaohang Weng^{1,2}, Hui Li^{1,2,*}, Yongbin Zhou³, Chengshuai Ren⁴, Songzhu Zhang^{1,2} and Liying Liu^{1,2}

¹ College of Forestry, Shenyang Agricultural University, Shenyang 110866, China; wxh571602@163.com (X.W.); zhangsz@syau.edu.cn (S.Z.); liuliyingsyau@163.com (L.L.)

² Research Station of Liaohe-River Plain Forest Ecosystem, Chinese Forest Ecosystem Research Network (CFERN), Shenyang Agricultural University, Tieling 110161, China

³ Institute of Modern Agricultural Research, Dalian University, Dalian 116622, China; yyzyb@163.com

⁴ Liaoning Water Conservancy and Hydropower Survey and Design Research Institute Co., Ltd., Shenyang 110055, China; rcs4307@163.com

* Correspondence: lihui@syau.edu.cn; Tel.: +86-15940526007

Abstract: The concentrations of exogenous nitrogen and calcium can significantly regulate plant growth and photosynthesis and mutually affect their absorption and utilization. However, whether there is an optimal nitrogen–calcium ratio (N:Ca ratio) in poplar seedling growth and physiological adaptation and what the mechanism of changes in the transcriptome is remain unclear. In this study, three different N:Ca ratios were used to grow poplar seedlings, and physiological and transcriptomic methods were used to study the molecular mechanisms of poplar growth under nitrogen–calcium synergy and to determine the optimal N:Ca ratio for poplar seedling growth. The results of this study showed that maximum poplar seedling growth occurred in the treatment with an N:Ca ratio of 2, which resulted in significantly greater induction of growth than the two other treatments ($p < 0.05$). Under the lowest N:Ca ratio, poplar seedlings can ensure normal development by regulating photosynthesis, while under the highest N:Ca ratio, regulating nitrogen metabolism can achieve the same result. These results contribute to a better understanding of the molecular mechanisms by which poplar seedlings respond to different ratios of N:Ca. This study provides a valuable basis for exploring the synergistic effects of nitrogen and calcium on the growth of poplar shelterbelts.

Keywords: N:Ca ratio; poplar seedlings; growth; photosynthetic; antioxidant enzyme activity; transcriptome



Citation: Weng, X.; Li, H.; Zhou, Y.; Ren, C.; Zhang, S.; Liu, L. Relative Availability of Nitrogen and Calcium Regulates the Growth of Poplar Seedlings Due to Transcriptome Changes. *Forests* **2023**, *14*, 1899. <https://doi.org/10.3390/f14091899>

Academic Editor: José Javier Peguero-Pina

Received: 30 August 2023

Revised: 13 September 2023

Accepted: 13 September 2023

Published: 18 September 2023



Copyright: © 2023 by the authors. Licensee MDPI, Basel, Switzerland. This article is an open access article distributed under the terms and conditions of the Creative Commons Attribution (CC BY) license (<https://creativecommons.org/licenses/by/4.0/>).

1. Introduction

Photosynthesis is essential for plant growth and ecosystem stability [1,2]. Through photosynthesis, plants use photosynthetic pigments to convert carbon dioxide (CO₂) and water into organic matter (carbohydrates) to provide energy for plant growth [3]. Nitrogen can not only change the direction of plant photosynthesis by regulating the shape and size of plant chloroplasts but also affect photosynthesis by affecting proteins (Calvin cycle proteins and thylakoid proteins) in plants and the accumulation of carbon in plants [4–6]. As a “second messenger”, calcium can ensure normal photosynthesis by regulating the expression of genes related to leaf gas exchange, the PSII process, carbohydrate metabolism, and chlorophyll synthesis [7,8]. Excessive Ca²⁺ can poison plants, leading to stomatal closure in leaves, damage to the chloroplast and thylakoid membranes, and interference with photosynthesis [9,10]. Calcium also regulates plant cell mitosis by controlling the distribution of calcium ions in the plant body and the number of receptors (calmodulin), affecting plant carbon and energy consumption [11,12]. Therefore, the interaction between nitrogen and calcium can maintain the integrity of cell structure and function and promote plant photosynthesis. Nitrogen form of the nitrogen compound and concentration

affect the uptake of calcium by plants, and calcium can also promote nitrogen uptake by increasing the activity of nitrogen-metabolizing enzymes in plant leaves [13,14]. Given the increasingly serious state of global nitrogen deposition [15–17] and the spatial heterogeneity of calcium [18,19], it is of great significance to further study the regulatory effects of the N:Ca ratio of applied treatment solutions to improve plant productivity and promote the cultivation of plantation forests.

Transcriptomics can identify valuable genes, reveal the molecular mechanisms of various biological functions and have groundbreaking significance in understanding the regulatory mechanisms of gene expression and environmental adaptation [20,21]. Much progress has been made in elucidating transcriptome regulation in the adaptation of some plants to physiological changes under different exogenous nitrogen concentrations [22,23]. For example, transcriptome analysis of *Arabidopsis thaliana* showed that under conditions of inadequate exogenous nitrogen supply, the upregulated genes were primarily enriched in amino acid metabolism, transport, and stress pathways, whereas the downregulated genes were enriched in hormone metabolism and REDOX reaction pathways [24]. Luo et al. [25] studied nitrogen starvation and excess in poplar and showed that a large number of gene ontology terms (GO terms) enriched in poplar root and leaf gene expression are related to development, nitrogen metabolism, stress response, and hormone stimulation. Calcium ions also play an important role in plant growth and development, and excess or depleted calcium ion concentrations interfere with the normal physiological function of plants [26,27]. However, recent studies on the molecular mechanism of calcium regulation of plant growth mainly focus on herbaceous plants or cash crops [28–30]. In studies exploring the effects of calcium stress on *Alfalfa* and *Arabidopsis* growth, experts found that differentially expressed genes were mainly concentrated in the abscisic acid, jasmonic acid, and oxalic acid production; calcium transport; and calcium balance pathways. Calcium-dependent protein kinase (CDPK) superfamily genes play an important role in coping with high calcium stress and calcium equilibrium pathways [31–33]. However, recent research on nitrogen and calcium application has mainly focused on the yield of cash crops [34,35] or the growth of other ornamental plants [36]. In their study, Ozyhar et al. [37] showed that combined N and Ca application can affect the absorption of other nutrient elements in poplar, thus promoting plant growth in acidic soil. The molecular mechanism for the regulation of plant growth by the N:Ca ratio, however, has yet to be investigated. Therefore, determining the responses of poplar seedling growth to the relative availability of nitrogen and calcium has a significant effect on improving plant productivity, enhancing the efficacy of shelterbelts and promoting ecological balance.

Populus spp. are able to survive on a variety of barren soils due to their high adaptability, and most can reproduce asexually, yield large amounts of seedlings, renew quickly, and have strong stress resistance [38,39]. The ecological function of poplar planting is to reduce erosion and runoff and to protect soil water content, so poplar has been widely planted as the main afforestation species in the Three-North shelterbelt [40,41]. However, due to the rapid growth of poplar, its short renewal cycle, and its high water consumption—coupled with the cultivation using a single method, the use of artificial forests; shelterbelts mostly being built in desert sand and hilly areas, poor site conditions, and low soil fertility—a decline in poplar plantation quality has occurred, and the special results showed that the growth of poplar decreased, the soil of forest land degraded, and the biodiversity weakened [42–44]. To date, studies on the effects of nutrient elements on poplar growth have mainly focused on single elements, such as available potassium [45,46], alkali-hydrolyzed nitrogen [47,48], soluble calcium [49], available phosphorus [46,50], and C:N:P stoichiometry [51]. However, there is a lack of attention to the value of the N:Ca ratio and its transcriptome. The objective of this study was to investigate the synergistic effect of the N:Ca ratio on poplar growth. The effects of three different N:Ca ratios on poplar seedling physiology and at the molecular level were compared. Finally, we combined transcriptomics techniques to analyze the molecular mechanism of the N:Ca ratio regulation of poplar growth. This study

provides a theoretical basis for the cultivation of poplar seedlings and the enhancement of shelterbelt function.

2. Materials and Methods

2.1. Plant Materials and Experimental Treatments

“Liao Hu No. 1” poplar (*P. simonii* × *P. euphratica*) seedlings were planted in a greenhouse at Shenyang Agricultural University, Liaoning, China, and this experiment was run from April to July 2019. The plants were grown in hydroponic pots with dimensions of 32 cm length × 18 cm width × 14 cm height filled with seven liters of nutrient solution. The 18 seedlings in 3 plastic pots (3 seedlings per pot) were divided into 3 groups. After 20 days of recovery, the lateral bud of each poplar seedling was treated so that only one lateral bud was selected for each seedling at the same position and treated with nitrogen and calcium.

Deionized water was used to formulate the nutrient solution following Xie [52]. The pH of the solution was maintained at 5–6 by adding NaOH. Calcium was provided by anhydrous CaCl₂; nitrogen was provided by NH₄Cl and NaNO₃ at a ratio of 1:1. Based on the results of previous studies (Figure S1), the concentration of Ca²⁺ was set 2.5, 5, and 10 mmol·L⁻¹, and the nitrogen concentration was set 10 mmol·L⁻¹. The treatments were configured together with N:Ca ratios of 1, 2, and 4 and labelled L (the lowest N:Ca ratio), O (the moderate N:Ca ratio), and H (the highest N:Ca ratio), respectively. Other compounds that provided a large number of elements were KCl, MgSO₄, KH₂PO₄, EDTA-Na₂, and FeSO₄, ensuring that the contents of P, K, Mg, and S in each treatment were 1.0, 6.0, 2.0, and 2.0 mmol·L⁻¹, respectively. Trace elements were provided by H₃BO₃, MnCl₂, CuSO₄, ZnSO₄, and H₂MoO₄. The above nutrient solution was proportionally dissolved in 7 L of ultrapure water and replaced every 5 days. After 50 days of treatment, leaves at similar positions were sampled from all treatments, immediately snap-frozen in liquid nitrogen, and sent to Shanghai Meiji Biomedical Technology Co., Ltd., Shanghai, China, for mRNA extraction and transcriptome sequencing analysis.

2.2. Measurement of Growth Indicators

The height and diameter of the base of the plant were measured using a tape measure and Vernier calipers to accuracies of 0.10 cm and 0.01 mm, respectively. The whole plant was washed, placed in an envelope, and then placed in an oven and dried at 65 °C to obtain a constant weight. An analytical balance accurate to 0.01 g was used to weigh the total plant biomass [49].

2.3. Measurement of Photosynthetic Indicators

At the peak of poplar seedling growth (July 2019), three seedlings were selected from each treatment using a Li-6400 photosynthesis meter (LI-COR, Inc., Lincoln, NE, USA) to measure the net photosynthetic rate (P_n), stomatal conductance (G_s), transpiration rate (T_r), and intercellular CO₂ concentration (C_i) [22]. During the vigorous growth period of the poplar seedlings, three seedlings were selected at random for each treatment, fresh leaves were harvested, the main veins were removed, 0.1 g was weighed and soaked in 98% ethanol for 48 h, and UV spectrophotometry was used for determination [53]. Approximately 0.5 g of poplar seedling dry sample (after ball milling) was placed in a centrifuge tube. The content of soluble sugars was determined using the 80% ethanol + anthrone colorimetric procedure, and starch was determined using the perchloric acid method + anthrone colorimetric procedure [53–56]. The detailed experimental operation can be found in the previous research methods of this research group [49].

2.4. Measurement of Antioxidant Enzyme Activity

For the determination of antioxidant enzymes, 0.4 g of samples was taken from fresh leaves, stored in a frozen pipe, fixed with liquid nitrogen, and stored in a refrigerator at –80 °C. At the time of measurement, samples were taken according to the mark and put

into a mortar. Then, 5 mL of precooled phosphate buffer was added, the sample was ground, the homogenate was centrifuged at 13,000 rpm at 4 °C for 15 min, and the supernatant was placed into a centrifuge tube for reserve (three repeats for each sample). The level of peroxidase (POD) was determined according to the guaiacol method (25 mM, pH = 7.0, include 0.1 mM EDTA PBS buffer + 1% guaiacol/ μ L + 20 mM H₂O₂/ μ L + Extraction proteins). The level of catalase (CAT) was determined on the basis of ultraviolet absorption by hydrogen peroxide (25 mM, pH = 7.0, include 0.1 mM EDTA PBS buffer + 100 mM H₂O₂/ μ L + extraction proteins). The superoxide dismutase (SOD) level was determined by methionine (50 mM pH = 7.8 PBS + 1.3 μ M riboflavin + 63 μ M NBT + 13 mM riboflavin methionine) [57].

2.5. RNA Isolation, Library Construction, and Sequencing

Total ribonucleic acid (RNA) was extracted from samples of poplar seedlings treated with different N:Ca ratios, and Nanodrop 2000 software was used to measure the extracted RNA concentration and purity. The integrity of the RNA was determined via agarose gel electrophoresis, and the RNA integrity number (RIN) values were determined using Agilent 2100. For a single library, the total amount of RNA needed was ≥ 1 μ g, the concentration was ≥ 35 ng/ μ L, optical density (OD) 260/280 was ≥ 1.8 , and OD260/230 was ≥ 1.0 . After qualified analysis, transcriptome sequencing was conducted. The 3' terminus of eukaryotic messenger ribonucleic acid (mRNA) has a polyA tail structure, and the mRNA can be separated from the total RNA via A-T base-pairing with polyA using Oligo (dT) magnetic beads. Fragmentation buffer was used to randomly separate mRNA fragments, and approximately 300 bp fragments were separated using magnetic beads. Random hexamers of six bases were added under the action of reverse transcriptase to synthesize a single-stranded cDNA using mRNA as a template, and then a stable double-stranded structure was formed through the synthesis of the double strand. The cDNA library was purified via terminal repair, adding an A tail, connecting sequencing joints, screening cDNA (250–300 bp), PCR amplification, and purification of the PCR product. Eventually, sequencing was performed using the Illumina NovaSeq 6000 platform [58]. The above steps were carried out at Shanghai Meiji Biomedical Technology Co., Ltd.

2.6. Differential Expression Gene (DEG) Analysis

The raw reads were filtered to obtain high-quality clean reads, and clean reads were aligned with reference genomes of *Populus euphratica* (<https://www.ncbi.nlm.nih.gov/genome/?term=Populuseuphratica>, GCF_000495115.1) (accessed on 12 March 2023) using TopHat2 v2.1.1 (<http://tophat.cbc.umd.edu/>). Based on the existing reference genomes, the mapped reads were assembled and spliced using the software Cufflinks 2.2.1 (<http://cole-trapnellab.github.io/cufflinks/>) for comparison with known genes. FPKM (fragments per kilobase per million reads) was used to quantify the level of gene expression. DEGseq2 1.24.0 (<http://bioconductor.org/packages/stats/bioc/DESeq2/>) was the software used for differential expression, which calculated differential expression according to the read count data compared to genes. This analysis method was based on the negative binomial distribution model. For significantly differentially expressed genes, the default filtering criteria were as follows: FDR < 0.05 and $|\log_2FC| \geq 1$. If a gene satisfied both of these conditions, it was considered to be a differentially expressed gene.

To obtain high-quality sequencing data (clean reads), the original sequencing data were filtered. Using the GO database (<http://www.geneontology.org/>), genes according to which they participated were classified into the biological process (BP), cellular component (CC), and molecular function (MF) categories. The KEGG database (Kyoto Encyclopedia of Genes and Genomes, <http://www.genome.jp/kegg/>) was used to classify the genes according to the participating pathways or functions. Similarly, the Goatools 0.6.5 software package (<https://github.com/tanghaibao/GOatools>) was used for the GO enrichment analysis of genes/transcripts as a function of gene concentration. KEGG pathway enrichment analysis was carried out for genes/transcripts in the gene set using the R language

script, and when the p value < 0.05 , the GO term or KEGG pathway was considered to be significantly enriched.

2.7. Quantitative Real-Time PCR (RT-qPCR) Analysis

On the basis of differential expression gene (DEG) analysis, two genes commonly expressed in the high N:Ca and low N:Ca ratio treatments but with opposite regulation patterns were selected, and Primer Premier 6.0 was used to design primers for each gene (Table S1). N:Ca ratio polymerase chain reaction (PCR) was carried out on a quantitative PCR instrument with Bori 9600plus fluorescence using ChamQ SYBR Colour qPCR Master Mix (2X). A $2^{-\Delta\Delta C_t}$ analysis was performed on gene expression.

2.8. Statistical Analysis

Excel2019 software was used for data processing. SPSS 22.0 software (SPSS, Chicago, IL, USA) single factor analysis of variance was used for statistical analysis of various physiological indicators in different treatment groups, and the Duncan method was used to analyze the differences between different treatment groups. GraphPad Prism 9.41 software was used for mapping. The results in the bar chart are expressed as the mean \pm standard error (SE) of three repetitions.

3. Results

3.1. Optimal N:Ca Ratio for Poplar Seedling Growth

Each column and table shows the mean \pm SE value ($n = 3$). Different capital letters indicate a significant difference between treatments of N:Ca addition ($p < 0.05$).

To explore whether there is an optimal N:Ca ratio for the growth of poplar seedlings, different N:Ca ratio treatments were carried out on poplar seedlings. With the increase in the N:Ca ratio, the plant height, basal diameter, and total biomass of poplar seedlings first increased and then decreased and reached the maximum value when the N:Ca ratio was 2 (Table 1). Photosynthesis is the most basic physiological phenomenon in plants and the only way to accumulate dry matter [59]. In this experiment, the photosynthetic parameters of poplar seedlings under different N:Ca ratios were measured. The values of the P_n , T_r , G_s , and C_i of poplar seedlings showed a trend of O (N:Ca ratio) $>$ H (N:Ca ratio) $>$ L (N:Ca ratio). When the N:Ca ratio was 2, the photosynthetic parameters reached the maximum value, and the difference between the other treatments reached a significant level ($p < 0.05$) (Figure 1a–d). Meanwhile, only the difference in the G_s index between the H (N:Ca ratio) and L (N:Ca ratio) treatments reached a significant level ($p < 0.05$). Since chlorophyll is a key indicator of plant growth, its content is closely linked to the capacity for photosynthesis [60]. Compared to the optimal nitrogen–calcium ratio, chlorophyll-a contents were reduced by 23.05% and 10.95% under the L (N:Ca ratio) and H (N:Ca ratio) treatments, respectively, and chlorophyll-b contents were reduced by 36.11% and 25.08%, respectively, with significant differences ($p < 0.05$) (Figure 1e,f). NSCs are storage substances that accumulate under the overproduction of plant carbohydrates or certain stress environments and are major energy substances in plant growth and metabolism as well as adaptation to extreme climates [61]. Compared to the optimal nitrogen–calcium ratio, soluble sugar content was reduced by 14.01% and 17.90% under the L (N:Ca ratio) and H (N:Ca ratio) treatments, respectively, and starch content was reduced by 22.54% and 20.67%, respectively, with significant differences ($p < 0.05$) (Figure 1g,h). The stress resistance of poplar under different N:Ca ratios was analyzed, and antioxidant enzyme activity indices under the L and H treatments were found to be significantly lower than those under the N:Ca ratio of 2 ($p < 0.05$) (Figure 2).

Table 1. Growth response to the value of N:Ca ratio in poplar seedlings.

	Plant Height (cm)	Basal Diameter (mm)	Biomass (g)
L (N:Ca ratio)	64.17 ± 1.934 C	7.33 ± 0.133 C	28.46 ± 0.382 C
O (N:Ca ratio)	74.93 ± 1.541 A	9.05 ± 0.241 A	33.54 ± 0.849 A
H (N:Ca ratio)	69.77 ± 0.736 B	8.12 ± 0.520 B	30.27 ± 0.613 B

Different terms (A, B, and C) within each column indicate that there are significant differences between the average values ($p \leq 0.05$).

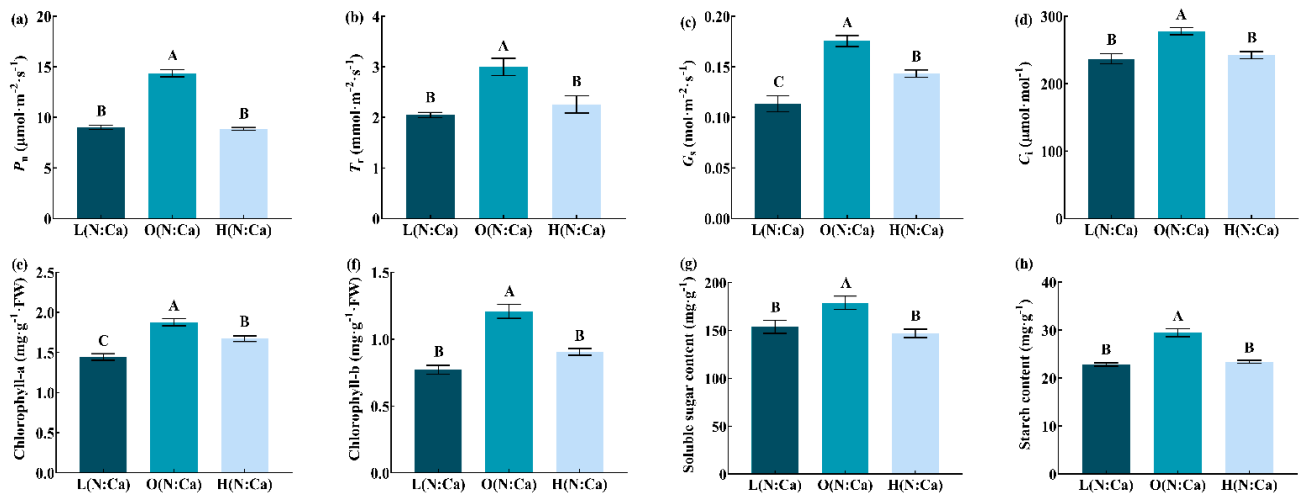


Figure 1. Photosynthetic response to the value of N:Ca ratio in poplar seedlings. Error bars are means \pm SE ($n = 3$), and different terms (A, B, and C) within each column indicate that there are significant differences between the average values ($p \leq 0.05$). (a) the net photosynthetic rate (P_n) of poplar seedling leaves response to the value of N:Ca ratio, (b) the transpiration rate (T_r) of poplar seedling leaves response to the value of N:Ca ratio, (c) the stomatal conductance (G_s) of poplar seedling leaves response to the value of N:Ca ratio, (d) the intercellular carbon dioxide concentration (C_i) of poplar seedling leaves response to the value of N:Ca ratio, (e) the chlorophyll-a content of poplar seedling leaves response to the value of N:Ca ratio, (f) the chlorophyll-b content of poplar seedling leaves response to the value of N:Ca ratio, (g) the soluble sugar content of poplar seedling leaves response to the value of N:Ca ratio, (h) the starch content of poplar seedling leaves response to the value of N:Ca ratio.

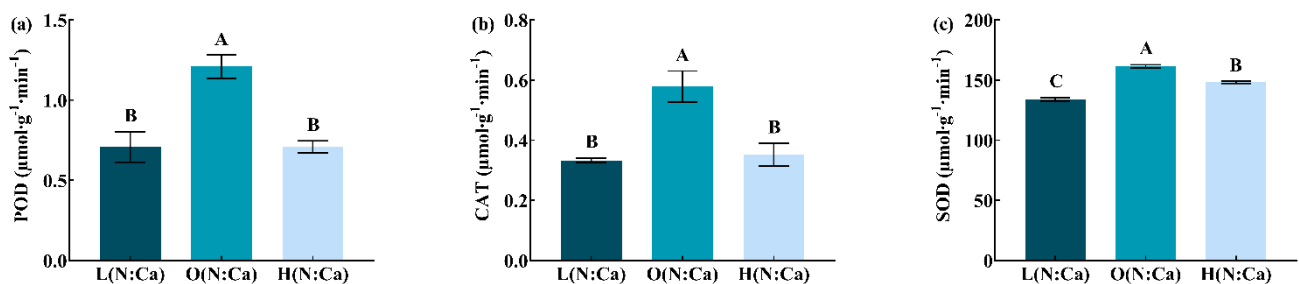


Figure 2. Antioxidant enzyme activity response to the value of N:Ca ratio in poplar seedlings. Error bars are means \pm SE ($n = 3$), and different terms (A, B, and C) within each column indicate that there are significant differences between the average values ($p \leq 0.05$). (a) the peroxidase (POD) of poplar seedling leaves activity response to the value of N:Ca ratio, (b) the catalase (CAT) of poplar seedling leaves activity response to the value of N:Ca ratio, (c) the superoxide dismutase (SOD) of poplar seedling leaves activity response to the value of N:Ca ratio.

3.2. Sequencing Data Filtering and Quality Control Analysis

Total RNA reads were extracted from poplar seedling leaves with the lowest N:Ca ratio (L1, L2, and L3), a moderate N:Ca ratio (O1, O2, and O3), and the highest N:Ca ratio (H1,

H2, and H3), and the original transcript data were obtained using Illumina. After screening and removing the original data for the sequenced joint sequences following filtering and removal of original joint sequence data, low-quality read segments, high N-rate sequences (N represents uncertain base information), and excessively short sequences, the number of effective clean reads obtained from each treatment was 58429284 (L1), 53655110 (L2), 61847128 (L3), 53709898 (O1), 53341884 (O2), 55631348 (O3), 56752418 (H1), 52776236 (H2), and 63511838 (H3), respectively, and the clean data from all samples were 7.9 Gb or greater. The error rate was less than 0.1%; Q20 and Q30 were more than 98.56% and 95.42%, respectively; and the GC contents were between 44.08% and 44.95%, respectively, which met the requirements for library construction (Table S2). String Tie software 1.3.3b was used to splice the sequencing data, and 78,404 transcripts were assembled. A total of 33,301 transcripts were longer than 1800 bp, accounting for 42.47% (Figure S2). The reference transcriptome sequencing data and splicing results for poplar treated with different N:Ca ratios are good, indicating that further transcriptomic analysis could be carried out.

3.3. Functional Annotation

The genes and transcripts were aligned with public protein databases such as GO, KEGG, COG, NR, Swiss-Prot, and Pfam. Genes and transcripts were aligned to publicly available protein databases such as the GO, KEGG, COG, NR, Swiss-Prot and Pfam databases. In total, 35,677 (94.31%) genes and 75,546 (96.35%) transcripts were successfully annotated (Table 2). Most of the genes and transcripts were annotated using the NR database (94.22% and 96.29%, respectively), followed by COG (88.99% and 92.14%, respectively), GO (75.54% and 75.81%, respectively), Swiss-Prot (75.40% and 78.17%, respectively), Pfam (73.13% and 74.64%, respectively), and KEGG (38.89% and 41.67%, respectively) (Table 2).

Table 2. Functional annotation of transcriptome data in six public protein databases.

	Gene Number (Percent)	Transcript Number (Percent)
GO	28,577 (75.54%)	59,440 (75.81%)
KEGG	14,713 (38.89%)	32,673 (41.67%)
COG	33,664 (88.99%)	72,240 (92.14%)
NR	35,644 (94.22%)	75,492 (96.29%)
Swiss-Prot	28,523 (75.4%)	61,291 (78.17%)
Pfam	27,665 (73.13%)	58,522 (74.64%)
Total annotation	35,677 (94.31%)	75,546 (96.35%)
Total	37,831 (100%)	78,404 (100%)

3.4. Mining the DEGs

The transcriptome data for the different treatments were compared and analyzed, and 7585 DEGs were filtered, among which 1,606,435, and 3363 unigenes were identified in H vs. O, L vs. O, and H vs. L, respectively. Among them, the number of different genes unique to the H vs. O, L vs. O, and H vs. L comparison groups was 384,105, and 1077, respectively, and the number of common DEGs among the three comparison groups was 8 (Figure 3d). Statistical difference analysis of gene expression levels was conducted. Generally, if the expression level of the same gene in one group of samples is twice or more than that in another group, it is considered that the gene has different expression levels in the two groups of samples [62]. Therefore, using DESeq2 software to p -adjust < 0.05 , $FC \geq 2$ is the criterion for filtering out the differentially expressed genes. A total of 2619 and 3816 unigenes [L vs. control (O)], 77 and 83 unigenes (H vs. O), and 2201 and 1162 unigenes (H vs. L) were identified with noticeable upregulation and downregulation, respectively (Figure 3a–c). It should be noted that the number of DEGs in poplar seedlings treated with the high N:Ca ratio was significantly lower than that in seedlings treated with the low N:Ca ratio, suggesting that a high N:Ca ratio may inhibit the expression of some genes in poplar seedlings. Additionally, Venn diagrams reveal unique and shared genes between

the groups [63], as shown in Figure 3d, there were 8 shared genes in total among the 3 different groups.

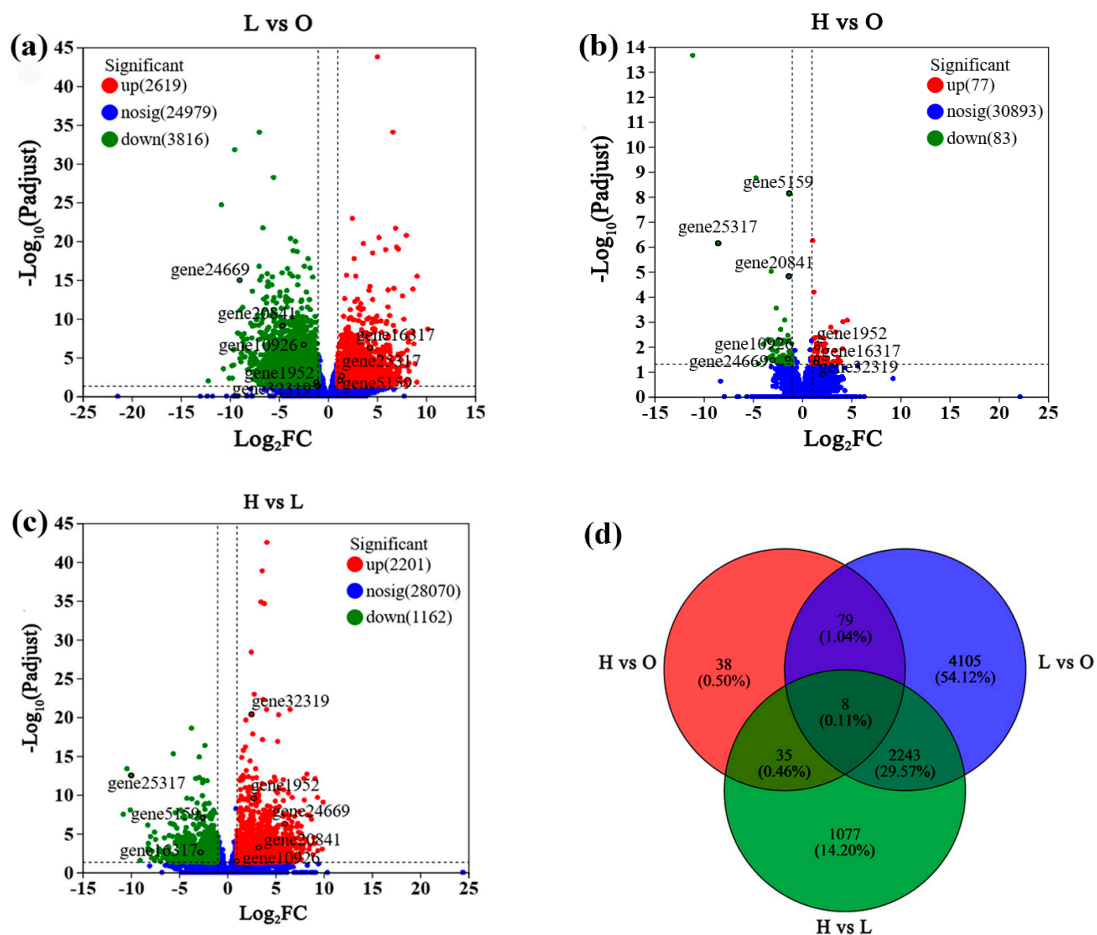


Figure 3. Numbers and distribution of upregulated and downregulated genes in different groups. (a) Volcano plot analysis of the DEGs in the L (the lowest nitrogen calcium ratio) vs. control (O) (the moderation nitrogen calcium ratio), (b) H (the highest nitrogen calcium ratio) vs. O, and (c) H vs. L groups. Red dots and green dots indicate significant up-regulation and down-regulation of differential gene expression, respectively ($p < 0.05$), and genes with insignificant differences are indicated by blue dots. The abscissa represents the change in gene expression multiples in different samples, whereas the ordinate represents the significance of the variation in gene expression. (d) Venn diagram between samples: Different-colored circles representing the number of common and unique genes among different gene sets. The sum of all the numbers in the circle represents the sum of the number of genes in the gene set, and the cross area of the circle represents the total number of genes in each gene set.

3.5. GO Enrichment Analysis of the DEGs

A GO enrichment histogram of the differentially expressed genes is a direct reflection of the distribution of the number of DEGs enriched in cellular elements, molecular functions, and biological processes and is used to perform enrichment analysis of GO terms annotated by DEGs [64]. When the lowest N:Ca ratio was compared to the medium N:Ca ratio, the top 20 Go-enriched biological processes accounted for 71.34%, and the cell components accounted for 24.70% (Figure 4a). The DEGs of biological processes are mainly concentrated in oligosaccharide biosynthesis, photosynthesis, and light harvesting of photosystem I. The cell components were mainly enriched in photosystem I and photosystem II, and the molecular function category includes only chlorophyll binding. Among the top 20 enriched GO terms, in the comparison of the highest N:Ca ratio with

the moderate N:Ca ratio, biological processes accounted for 83.25% of the DEGs, and the DEGs were predominantly enriched in the reactive nitrogen species metabolic process, nitrate metabolic process, and nitrate assimilation. The molecular function category only contained the unfolded protein binding function, and the cellular component accounted for 14.83% of the DEGs, which were mainly enriched in the chloroplast (Figure 4b). Consistent with the previous results, a directed acyclic graph (DAG) showed significant enrichment of plastoglobule, photosystem I, and chlorophyll binding in poplar treated with the lowest N:Ca ratio (Figure 4c) and nitrate assimilation, nitrate metabolic process, and nitrate assimilation in poplar treated with the highest N:Ca ratio (Figure 4d).

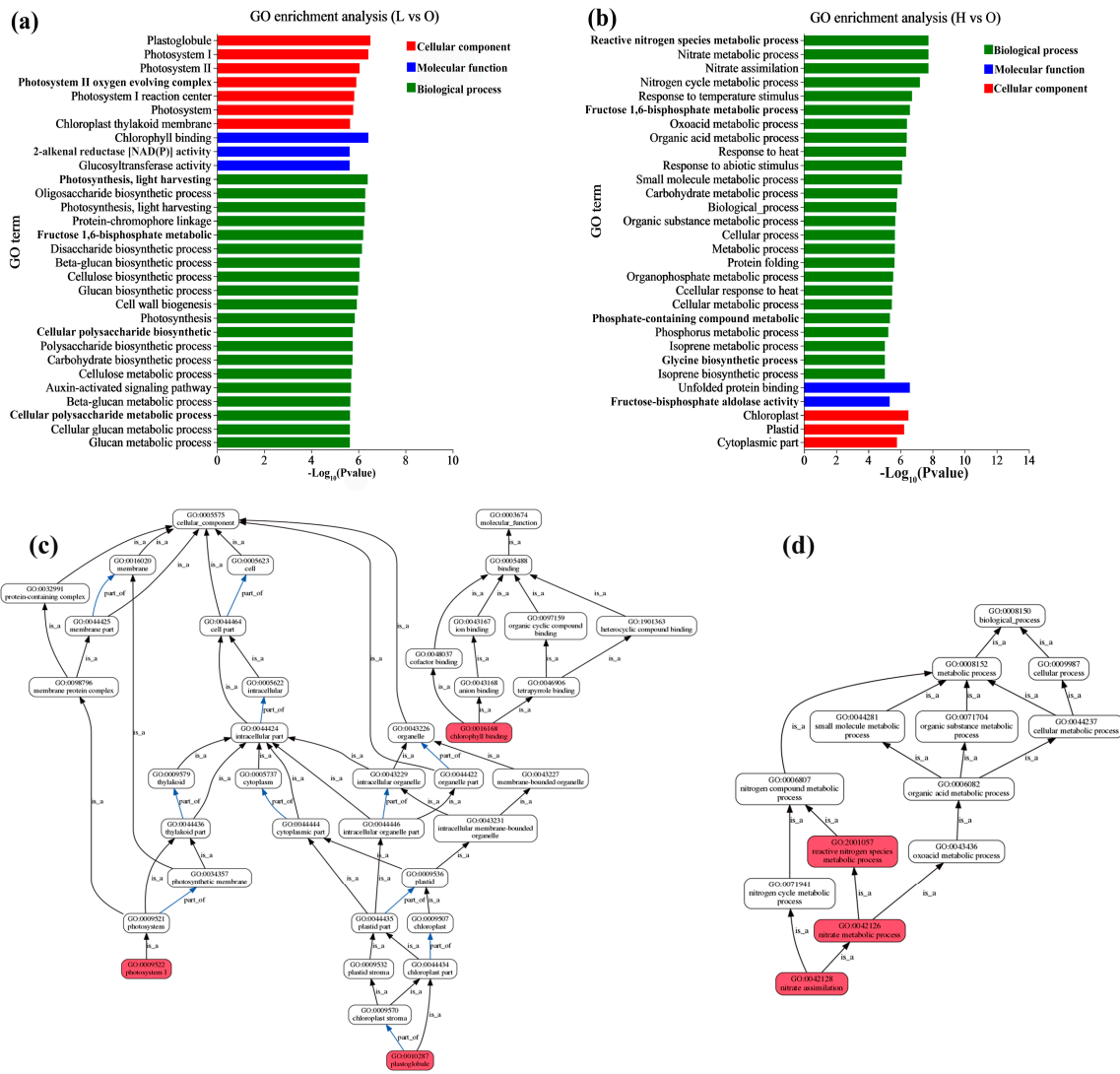


Figure 4. GO enrichment analysis of the DEGs. (a,b) are the DEGs’ enrichment when comparing low and high N:Ca ratios, respectively, to the optimal N:Ca ratio. The vertical axis represents the GO term, and the horizontal axis represents the enrichment significance level; the smaller the FDR, the larger the $-\log_{10}(p\text{-value})$ value and the more significantly enriched the GO term. The three colors represent three categories, namely biological processes (BP), cellular components (CC), and molecular functions (MF). (c,d) are a DAG map that shows the GO enrichment of DEGs when comparing low and high N:Ca ratios, respectively, to the optimal N:Ca ratio. Each box represents a GO term, and the color box shows the GO term with significant enrichment in the gene set. The closer the color is to red, the more significantly the GO term is enriched; the line between GO terms indicates the relationship between the two GOs.

3.6. Analysis of Metabolism and Regulatory Pathways

Comparative analysis of the DEGs among the three groups (L vs. O and H vs. O) can provide potential information regarding the molecular mechanism of the poplar response to treatments with different N:Ca ratios. Among the top 20 KEGG analysis results, the five most significantly enriched DEGs in L vs. O were photosynthesis (map00195), plant hormone signal transduction (map04075), starch and sucrose metabolism (map00500), carbon fixation in photosynthetic organisms (map00710), and photosynthesis–antenna proteins (map00196) (Figure 5a). In contrast, in the H vs. O KEGG enrichment analysis, only 13 pathways were consistent with a *p* value < 0.05, and the five most significantly enriched DEGs in H vs. O were the pentose phosphate pathway (map00030), protein processing in the endoplasmic reticulum (map04141), carbon fixation in photosynthetic organisms (map00710), glyoxylate and dicarboxylate metabolism (map00010), and fructose and mannose metabolism (map00051) (Figure 5b). These DEGs in both L vs. O and H vs. O were differentially enriched in glyoxylate and dicarboxylate metabolism, glycolysis/gluconeogenesis, fructose and mannose metabolism, alanine, aspartate and glutamate metabolism, and carbon fixation in photosynthetic organisms. These metabolic pathways include photosynthetic and respiratory pathways. It was found that *gene12251*, *gene9460*, *gene18199*, and the other nine differentially expressed genes were obviously upregulated when the ratio of nitrogen to calcium was the highest or the lowest in order to regulate the carbon cycle of poplar seedlings (Figure 6).

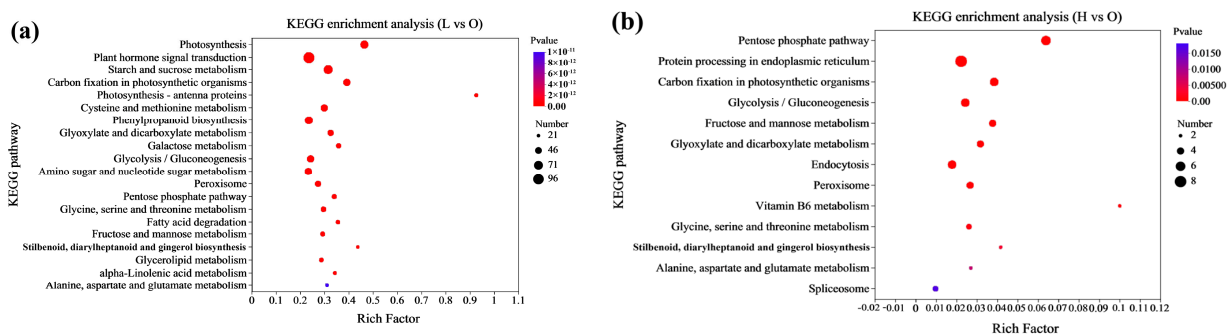


Figure 5. KEGG enrichment analysis of the DEGs. The vertical axis indicates the name of the pathway, the horizontal axis indicates Rich factor, the size of the dots indicates the number of genes in this pathway, and the colors of the dots correspond to different *p*-value ranges. (a) are the DEGs’ KEGG enrichment when comparing low N:Ca ratios to the moderate N:Ca ratio, (b) are the DEGs’ KEGG enrichment when comparing high N:Ca ratios to the moderate N:Ca ratio.

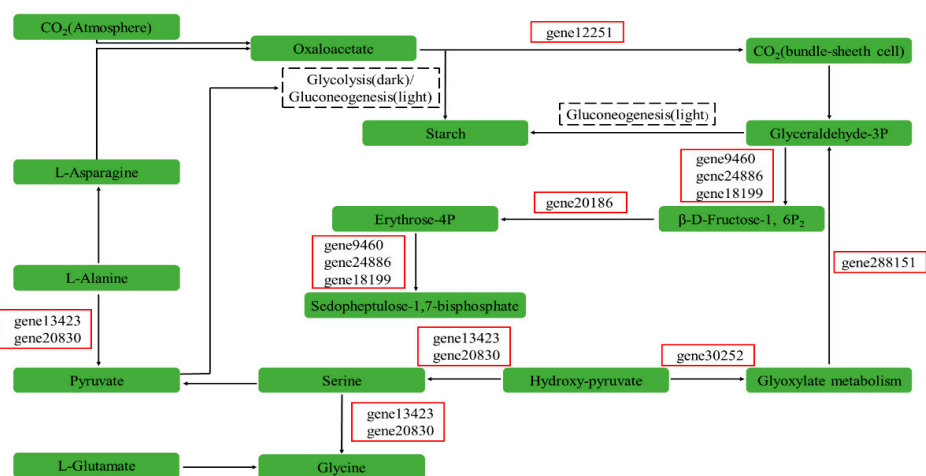


Figure 6. Expression of genes related to carbon cycling in poplar seedling leaves under the value of N:Ca ratio. The red box represents the gene name, the arrows represent metabolic processes; and the dashed black lines represent metabolic pathways.

3.7. RT-qPCR Validation of DEGs

The results of the transcriptome data analysis were verified via qRT-PCR (Figure 7). Four differentially expressed genes were randomly selected: gene5159 (universal stress protein A-like protein), gene25317 (E3 ubiquitin-protein ligase UPL5-like, transcript variant X1), gene1952 (SWR1-complex protein 4-like), and gene32319 (receptor-like serine/threonine-protein kinase SD1-8). The results showed that although there were some differences in the degree of upregulation or downregulation of expression determined by RNA-seq and qRT-PCR, the expression trends of the genes reflected by the qRT-PCR results were consistent with the transcriptome sequencing results, which may be related to the detection range and expression calculation methods of the two methods. In conclusion, the transcriptome sequencing data for poplar seedlings treated with different N:C ratios are accurate and reliable.

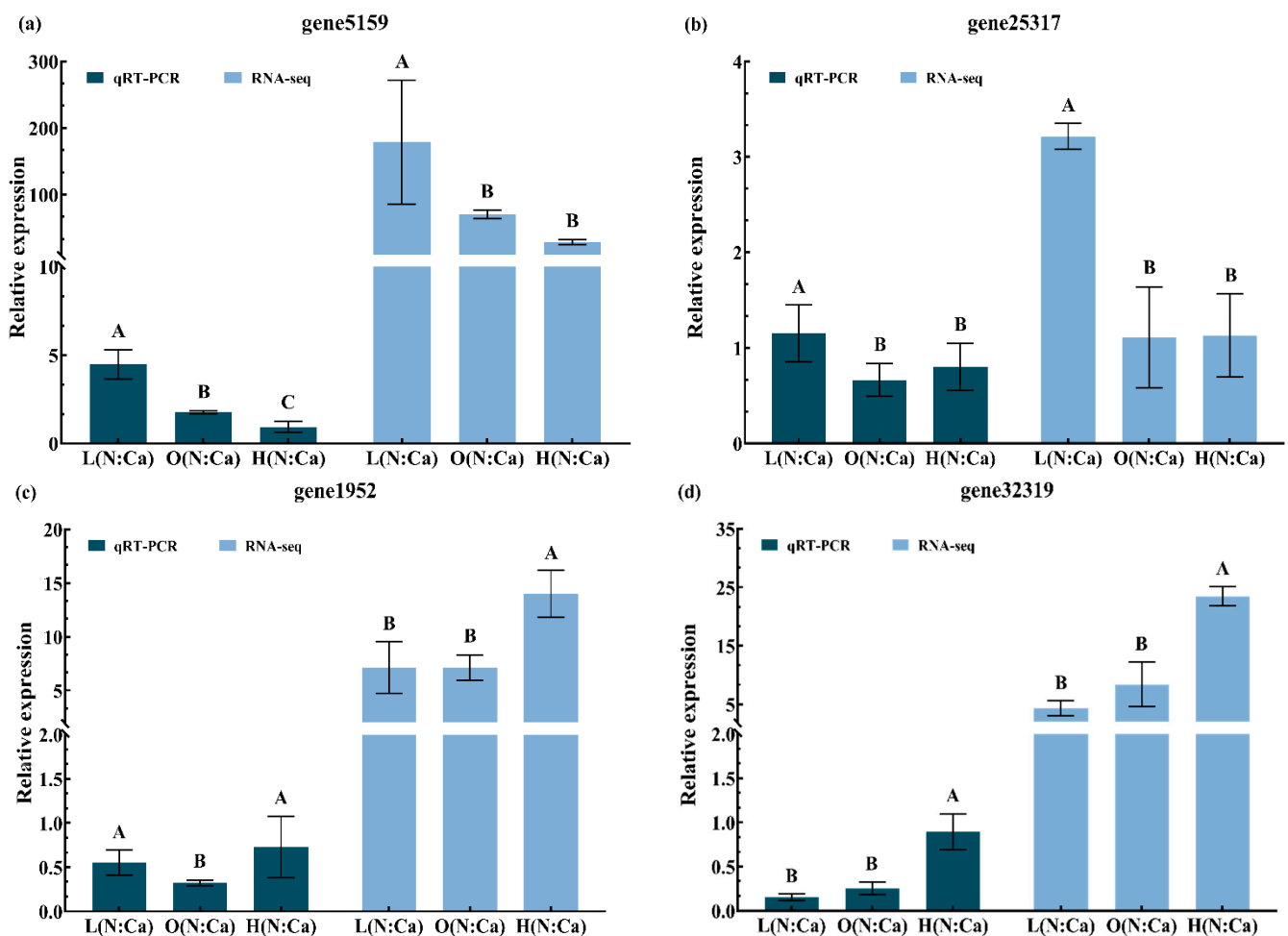


Figure 7. qRT-PCR validation of relative expression levels of DEGs. Error bars are means \pm SE ($n = 3$), and different terms (A, B, and C) within each column indicate that there are significant differences between different treatments under the same test method ($p \leq 0.05$). (a) is relative expression of *gene 5159* under different test methods, (b) is relative expression of *gene 25317* under different test methods, (c) is relative expression of *gene 1952* under different test methods, (d) is relative expression of *gene 32319* under different test methods.

4. Discussion

4.1. An Optimal N:Ca Ratio Exists for Poplar Seedling Growth

Plant nitrogen obtained from soil, primarily in the form of nitrate and ammonium, has been shown to play a dominant role in growth and development [65]. It accounts for 1%–4% of the plant's dry matter and combines with compounds produced by the metabolism

of carbohydrates to form amino acids and proteins [66]. As an essential component of protein, nitrogen is involved in all major processes that affect plant development and yield formation [67]. At the same time, the content of exogenous calcium can affect the absorption and utilization of other nutrients, such as nitrogen [68]. Calcium is essential for plant growth and development under both non-stressed and stressed conditions, and it has multiple functions [69]. First, calcium is important for the stability of cell walls and membranes [70,71]. Second, calcium acts as a second messenger for plant growth and development, relieving plants from biotic stresses [72–74]. Meanwhile, the addition of calcium also improves the absorption of nitrogen by plants [75,76]. Fenn et al. [77] showed that the combined application of urea and calcium fertilizers significantly increased crop yield compared to the addition of either nitrogen fertilizers or calcium fertilizers alone, and calcium ions in the plants may promote ammonium nitrogen uptake by plants. Fu et al. [78] conducted a study on Pingyi sweet tea and found that the aboveground (leaf biomass and leaf area) and belowground (root biomass and root activity) growth of Pingyi sweet tea seedlings peaked when the N:Ca ratio was 2 to 3. In their study of peanuts, Zhang et al. [35] conducted experiments with different levels of nitrogen and calcium and found that the peanut leaf net photosynthetic rate peaked under 25% nitrogen reduction and 300 kg·hm⁻² calcium fertilizer application conditions. According to Zou et al. [79], when the nitrogen concentration was 0.2 g·kg⁻¹ and the calcium concentration was 1 g·kg⁻¹, the antioxidant enzymatic activity of flue cured tobacco peaked, and the stress-relieving capacity was highest at this time. Consistent with the above studies, the synergism of nitrogen and calcium can improve photosynthesis and stress resistance in poplar and promote the growth of poplar seedlings (Table 1, Figures 1 and 2). At the same time, there was a significant or extremely significant correlation between the physiological indicators (Table 3). The reasons for these findings can be roughly divided into three possibilities: first, once the nitrogen and calcium ion concentrations reach equilibrium, reducing the influence of the lowest or the highest concentration of nitrogen or calcium on the uptake of other nutrients into plants, the inhibition of protein synthesis of ribulose biphosphate carboxylase caused by an improper nitrogen supply of nutrition imbalance is alleviated, which is conducive to the recovery of photosynthesis. A second possible reason is that the nitrogen and calcium balance improves the integrity and stability of the chloroplast structure, enhances the activities of RuBisCO and phosphoenolpyruvate (PEP) carboxylase and thus improves the efficiency of carbon dioxide carboxylation and the activity of membrane ATPase, thereby improving the photosynthetic level of plants. A third potential explanation is the increased chlorophyll content, which promotes plant photosynthesis [80–82]. In summary, our results indicate that there is an optimal N:Ca ratio for poplar seedling growth, and these samples are suitable for further transcriptome comparative analysis.

Table 3. Pairwise correlations between all measured parameters.

	Plant Height	Basa Diameter	Biomass	Pn	Tr	Gs	Ci	Chlorophyll-a	Chlorophyll-b	Soluble Sugar	Starch Content	POD	CAT	SOD
Plant height	1													
Basal diameter	0.831 **	1												
Biomass	0.827 **	0.897 **	1											
Pn	0.765 *	0.801 **	0.904 **	1										
Tr	0.751 *	0.927 **	0.876 **	0.830 **	1									
Gs	0.845 **	0.855 **	0.918 **	0.809 **	0.816 **	1								
Ci	0.798 **	0.726 *	0.920 **	0.912 **	0.785 *	0.865 **	1							
Chlorophyll-a	0.904 **	0.910 **	0.836 **	0.777 *	0.812 **	0.889 **	0.697 *	1						
Chlorophyll-b	0.831 **	0.821 **	0.975 **	0.918 **	0.820 **	0.937 **	0.960 **	0.824 **	1					
Soluble sugar	0.424	0.65	0.745 *	0.827 **	0.732 *	0.728 *	0.772 *	0.524	0.759 *	1				
Starch content	0.701 *	0.798 *	0.935 **	0.953 **	0.861 **	0.852 **	0.899 **	0.777 *	0.946 **	0.832 **	1			
POD	0.820 **	0.698 *	0.822 **	0.937 **	0.694 *	0.805 **	0.909 **	0.743 *	0.873 **	0.741 *	0.834 **	1		
CAT	0.725 *	0.750 *	0.921 **	0.920 **	0.786 *	0.720 *	0.906 **	0.663	0.901 **	0.683 *	0.910 **	0.821 **	1	
SOD	0.852 **	0.884 **	0.948 **	0.827 **	0.789 *	0.928 **	0.806 **	0.922 **	0.927 **	0.612	0.871 **	0.773 *	0.810 **	1

*, $p < 0.05$; **, $p < 0.01$.

4.2. The Nitrogen–Calcium Ratio Regulates Different Plant Growth GO Terms

Transcriptomics can reveal the molecular mechanisms of a variety of biological functions during plant growth and provide improved genetic resources for plant breeding [83]. Investigating the mechanism of regulation of various nutrient elements on plant growth by transcriptomics provides a theoretical basis and guidance for improving plant productivity, restoring ecological balance, and promoting economic development [84–88]. GO analysis can provide a standardized vocabulary for the functional assignment of uncharacterized sequences [89], so it was used for the functional classification of poplar genes. The GO functional analysis under nitrogen stress showed that the main enriched GO terms were photosynthesis, biosynthesis of organic hydroxyl compounds, and biosynthesis of secondary metabolites [90]. During nitrogen deficiency, differentially expressed genes were mainly concentrated in cells, cell parts, membranes, and organs, as well as in binding and catalytic activities. Of these, protein metabolism, amino acid metabolism and photosynthesis were found to be significantly affected by nitrogen stress [91]. In contrast, the expression of some key genes involved plant amino acid metabolism (*NIA2*, *GDH2*, and *ASN1*) was significantly upregulated under high-nitrogen conditions [25]. As a nutrient element essential for plant growth and development, calcium is involved in a variety of cellular metabolic processes [92]. Ligaba-Osena et al. [93] showed that under low calcium concentrations, GO analysis highlighted the significant enrichment of several Ca^{2+} transporters, signaling genes, genes with transport activities, ATPase activity, catalytic activities, etc. Wang et al. [84] found that the application of exogenous calcium increased the proline and soluble sugar content in tea (*Camellia sinensis*) and improved heat resistance by enhancing heat stress signal transduction to mitogen-activated protein kinase terms. Liu et al. [94] found in a transcriptome analysis of *Parachlorella kessleri* that under received high calcium stress, the BP terms with the most genes were “cellular process” and “metabolic process”. The “cellular anatomical entity” was enriched by most genes in CC categories. In MF, the terms “binding” and “catalyst activity” were most common. In this study, the transcriptome of poplar seedlings was compared and analyzed. The findings of the current study were consistent with those of the studies mentioned above. The aim of this study was to compare and analyze the transcriptome of poplar seedlings. It was found that the most abundant terms among the differentially expressed genes in the L vs. O comparison in the BP class were photosynthesis and light collection in the photosystem. Oligosaccharide biosynthesis technology. In MF, the differentially expressed genes were mainly related to chlorophyll binding. In CC, the differentially expressed genes were mainly concentrated in terms related to photosynthesis (Figure 4a). In the H vs. O comparison, the most enriched BP gene pathways were the active nitrogen metabolism pathway and nitrate metabolism and assimilation. In addition, there was enrichment in terms of response to temperature stimulation, response to heat, and cellular processes. Unfolded protein binding and fructose-diphosphate carboxylase activity were the most enriched in the MF class. In CC, the differentially expressed genes were mainly concentrated in chloroplast and plastid related terms (Figure 4b). These results indicated that the growth and development of poplar seedlings were mainly regulated by Ca-related genes when the N:Ca ratio was low, while the growth and development of poplar seedlings were mainly regulated by N-related genes when the N:Ca ratio was high. At the same time, sufficient nitrogen content can activate some calcium-related action pathways, such as cellular processes. In addition, volcano plot analysis of L vs. O and H vs. O showed that *gene5159*, *gene25317*, *gene1952*, and *gene32319* had opposite regulatory trends (Figure 3a,b). Consistent with the results of the GO enrichment analysis, *gene5159* and *gene25317* were upregulated when the N:Ca ratio was low, which mainly affected the signal transduction mechanism, general stress proteins, proteolysis, endocytosis, and ubiquitin-protein ligase. *Gene1952* and *gene32319* were upregulated when the ratio of nitrogen to calcium was high and mainly acted on protein serine and threonine collecting activity, ATP binding activity, the plasma membrane, transmembrane protein tyrosine kinase, and protein phosphorylation.

4.3. Nitrogen–Calcium Synergies Activate Metabolic Pathways Related to Photosynthesis, Respiration, and Antioxidant Activity

KEGG enrichment can better highlight pathways involved in signaling and stress responses [95]. KEGG pathway analysis under nitrogen stress indicated that the DEGs were primarily involved in secondary metabolite photosynthesis and biosynthesis [92]. Nitrate reductase (NR) and glutamine synthetase (GS) play a key role in nitrogen metabolism during the conversion of inorganic to organic nitrogen [96]. Increased expression levels of GS and NR were conducive to the reduction of nitrate and the reassimilation of catabolism-derived ammonia, which increased the nitrogen assimilation efficiency and was conducive to improved photosynthetic ability [97]. Studies have found that in the absence of nitrogen, the *Pet* and *Psb* gene families are downregulated, inhibiting photosynthetic electron transfer and the PSII pathway, and the photosynthetic rate is reduced [98]. In *Arabidopsis*, Shi et al. [91] showed that under low nitrogen conditions, the primarily enriched KEGG pathways were eukaryotic ribosome synthesis, photosynthesis antenna protein, plant hormone signal transduction, phenylalanine metabolism, nitrogen metabolism, and amino acid metabolism and that there were variable splicing events. In studies on perennial ryegrass, KEGG enrichment analysis indicated that “photosynthesis-antenna protein” may have a positive response to appropriate nitrogen conditions, while “steroid biosynthesis”, “carotenoid biosynthesis”, and “c5 bis metabolism” are the most significantly enriched pathways in response to excess nitrogen [99]. Meanwhile, Ca²⁺ deficiency affects plant growth and mineral accumulation by regulating the transcription of Ca²⁺ transporter, Ca²⁺-binding protein, and Ca²⁺-dependent protein kinase and signaling genes [93]. Photosynthetic metabolism is one of the most enriched KEGG pathways in plants under high calcium stress. In the photosystem and electron transport system, 53 genes were significantly upregulated, and 5 genes were significantly downregulated ($p < 0.05$). In the process of carbon sequestration, the expression of 48 genes was significantly upregulated, and that of 19 genes was significantly downregulated [97]. The results of the present study are consistent with the findings of previous studies. Analysis of KEGG enrichment in poplar seedlings showed that the top five DEGs in the L vs. O comparison were photosynthesis, transduction of plant hormone signals, metabolism of starch and sucrose, carbon fixation in photosynthetic organisms, and photosynthetic antennal proteins (Figure 5a). The most significant differences in the H vs. O KEGG enrichment analysis, however, were the pentose phosphate route, processing of proteins in the endoplasmic reticulum, fixation of carbon in photosynthetic organisms, metabolism of glyoxylate and dicarboxylate, and metabolism of fructose and mannose (Figure 5b). Similarly, in the present study, differentially expressed genes were found to regulate metabolic pathways related to photosynthesis and respiration to maintain carbon balance in poplar seedlings when different N:Ca ratios produce stress (Figure 6) and promote plant growth via regulation. In conclusion, through transcriptome analysis, we confirmed that the synergy of nitrogen and calcium can promote the growth of poplar seedlings by regulating the progress of photosynthesis, promoting the accumulation of photosynthates, and improving the activity of antioxidant enzymes.

5. Conclusions

In summary, physiological and transcriptome analyses of poplar seedlings leaves were compared under the lowest N:Ca ratio, the moderate N:Ca ratio, and the highest N:Ca ratio. Different N:Ca ratios influenced plant growth and physiological characteristics, the concentration of nitrogen and calcium, and the activities of SOD, POD, and CAT in poplar seedlings, and the optimum N:Ca ratio of poplar seedlings was 2. DEGs were also influenced by different N:Ca ratio conditions in poplar. Poplar seedlings through regulated photosynthesis, respiration, and nitrogen metabolism pathways to respond to the different N:Ca ratio environments. To our best knowledge, we first provided a mechanism of N:Ca ratio for the poplar seedlings' development. These results provide a broader and better understanding of the processes underlying different N:Ca ratio responses and provide a foundation for improving the efficiency of nitrogen and calcium use in poplar.

Supplementary Materials: The following supporting information can be downloaded at: <https://www.mdpi.com/article/10.3390/f14091899/s1>, Table S1: Reaction primers and conditions; Table S2: Statistical table of sequencing data of “Liaohu No. 1” Poplar seedlings; Figure S1: Effects of combined application of nitrogen and calcium on growth and physiological characteristics of poplar seedlings; Figure S2: Transcript length distribution bar graph; Figure S3: Pearson correlations between all samples; Figure S4: GO and KEGG annotation classification statistics.

Author Contributions: H.L.: conceptualization, supervision, funding acquisition. X.W.: methodology, validation, formal analysis, investigation, writing—original, visualization. Y.Z.: conceptualization, supervision, C.R.: Investigation, S.Z.: Writing—review and editing; L.L.: Writing—review and editing. All authors have read and agreed to the published version of the manuscript.

Funding: This work was supported by the National Natural Science Foundation of China (31700552, 41450007, 31800364, and 31400611) and the Doctoral Research Startup Fund (880416020).

Data Availability Statement: The data presented in this study are available on request from the corresponding author. The data are not publicly available due to the policy of the institute.

Acknowledgments: We thank Huo Yan for his help in the operation of this experiment, and we thank Megi Bio for providing technical support.

Conflicts of Interest: The authors declare no conflict of interest.

References

1. Lawlor, D.W. Photosynthesis, productivity and environment. *J. Exp. Bot.* **1995**, *46*, 1449–1461. [[CrossRef](#)]
2. Li, H.; Li, X.; Zhang, G.; Weng, X.; Huang, S.; Zhou, Y.; Zhang, S.; Liu, L.; Pei, J. The Optimum Calcium Concentration for Seedling Growth of Mongolian Pine (*Pinus sylvestris* Var. *Mongolica*) Under Different Soil Types in Northern Semi-Arid Areas of China. *Front. Environ. Sci.* **2022**, *10*, 812. [[CrossRef](#)]
3. Goswami, R.K.; Agrawal, K.; Mehariya, S.; Molino, A.; Musmarra, D.; Verma, P. Microalgae-based biorefinery for utilization of carbon dioxide for production of valuable bioproducts. In *Chemo-Biological Systems for CO₂ Utilization*; CRC Press: Boca Raton, FL, USA, 2020; pp. 203–228. [[CrossRef](#)]
4. Evans, J.R. Photosynthesis and nitrogen relationships in leaves of C3 plants. *Oecologia* **1989**, *78*, 9–19. [[CrossRef](#)] [[PubMed](#)]
5. Liang, Y.; Wang, J.; Zeng, F.; Wang, Q.; Zhu, L.; Li, H.; Guo, N.; Chen, H. Photorespiration regulates carbon–nitrogen metabolism by magnesium chelatase d subunit in rice. *J. Agric. Food Chem.* **2020**, *69*, 112–125. [[CrossRef](#)]
6. Cai, Y.; Zhang, J.S.; Cai, C.; Zhu, C.W. Effects of elevated CO₂ concentration on photosynthesis of rice leaves under different nitrogen supply forms. *Soils* **2021**, *53*, 265–271. [[CrossRef](#)]
7. Zhang, Z.; Wu, P.; Zhang, W.; Yang, Z.; Liu, H.; Ahammed, G.J.; Cui, J. Calcium is involved in exogenous NO-induced enhancement of photosynthesis in cucumber (*Cucumis sativus* L.) seedlings under low temperature. *Sci. Hortic.* **2020**, *261*, 108953. [[CrossRef](#)]
8. Li, H.; Huo, Y.; Weng, X.; Zhou, Y.; Sun, Y.; Zhang, G.; Songzhu, Z.; Liu, L.; Pei, J. Regulation of the growth of Mongolian pine (*Pinus sylvestris* var. *mongolica*) by calcium–water coupling in a semiarid region. *Ecol. Indic.* **2022**, *137*, 108736. [[CrossRef](#)]
9. Brodribb, T.J.; McAdam, S.A.M. Unique responsiveness of angiosperm stomata to elevated CO₂ explained by calcium signalling. *PLoS ONE* **2013**, *8*, e82057. [[CrossRef](#)]
10. Mir, I.R.; Gautam, H.; Anjum, N.A.; Masood, A.; Khan, N.A. Calcium and nitric oxide signaling in plant cadmium stress tolerance: A cross talk. *S. Afr. J. Bot.* **2022**, *150*, 387–403. [[CrossRef](#)]
11. Siqueira, J.A.; Hardoim, P.; Ferreira, P.C.; Nunes-Nesi, A.; Hemerly, A.S. Unraveling interfaces between energy metabolism and cell cycle in plants. *Trends Plant Sci.* **2018**, *23*, 731–747. [[CrossRef](#)]
12. Winnicki, K. The winner takes it all: Auxin—The main player during plant embryogenesis. *Cells* **2020**, *9*, 606. [[CrossRef](#)]
13. Kaya, C.; Aydemir, S.; Akram, N.A.; Ashraf, M. Epibrassinolide application regulates some key physio-biochemical attributes as well as oxidative defense system in maize plants grown under saline stress. *J. Plant Growth Regul.* **2018**, *37*, 1244–1257. [[CrossRef](#)]
14. Souri, M.K.; Hatamian, M. Amino-chelates in plant nutrition: A review. *J. Plant Nutr.* **2019**, *42*, 67–78. [[CrossRef](#)]
15. Dentener, F.; Vet, R.; Dennis, R.L.; Du, E.; Kulshrestha, U.C.; Galy-Lacaux, C. Progress in monitoring and modelling estimates of nitrogen deposition at local, regional and global scales. In *Nitrogen Deposition, Critical Loads and Biodiversity*; Springer: Berlin/Heidelberg, Germany, 2014; pp. 7–22. [[CrossRef](#)]
16. Wen, Z.; Xu, W.; Li, Q.; Han, M.; Tang, A.; Zhang, Y.; Luo, X.; Shen, J.; Wang, W.; Li, K.; et al. Changes of nitrogen deposition in China from 1980 to 2018. *Environ. Int.* **2020**, *144*, 106022. [[CrossRef](#)] [[PubMed](#)]
17. Elrys, A.S.; Wang, J.; Metwally, M.A.; Cheng, Y.; Zhang, J.B.; Cai, Z.C.; Müller, C. Global gross nitrification rates are dominantly driven by soil carbon-to-nitrogen stoichiometry and total nitrogen. *Glob. Chang. Biol.* **2021**, *27*, 6512–6524. [[CrossRef](#)] [[PubMed](#)]

18. Fraterrigo, J.M.; Turner, M.G.; Pearson, S.M.; Dixon, P. Effects of past land use on spatial heterogeneity of soil nutrients in southern appalachian forests. *Ecol. Monogr.* **2005**, *75*, 215–230. [[CrossRef](#)]
19. Liu, J. Study on the Spatial Heterogeneity of Calcium in Soil and Plants in Typical Karst Dry-Hot Valley Mountain Area. Master's Thesis, Guizhou Normal University, Guiyang, China, 2022. [[CrossRef](#)]
20. Menz, J.; Li, Z.; Schulze, W.X.; Ludewig, U. Early nitrogen-deprivation responses in Arabidopsis roots reveal distinct differences on transcriptome and (phospho-) proteome levels between nitrate and ammonium nutrition. *Plant J.* **2016**, *88*, 717–734. [[CrossRef](#)]
21. Liu, G.; Liu, J.; Zhang, C.; You, X.; Zhao, T.; Jiang, J.; Chen, X.; Zhang, H.; Yang, H.; Zhang, D.; et al. Physiological and RNA-seq analyses provide insights into the response mechanism of the Cf-10-mediated resistance to *Cladosporium fulvum* infection in tomato. *Plant Mol. Biol.* **2018**, *96*, 403–416. [[CrossRef](#)]
22. Fang, X.; Li, Y.; Nie, J.; Wang, C.; Huang, K.; Zhang, Y.; Zhang, Y.; She, H.; Liu, X.; Ruan, R.; et al. Effects of nitrogen fertilizer and planting density on the leaf photosynthetic characteristics, agronomic traits and grain yield in common buckwheat (*Fagopyrum esculentum* M.). *Field Crop. Res.* **2018**, *219*, 160–168. [[CrossRef](#)]
23. Duan, Y.; Yang, H.; Yang, H.; Wu, Y.; Fan, S.; Wu, W.; Lyu, L.; Li, W. Integrative physiological, metabolomic and transcriptomic analysis reveals nitrogen preference and carbon and nitrogen metabolism in blackberry plants. *J. Plant Physiol.* **2023**, *280*, 153888. [[CrossRef](#)]
24. Krapp, A.; Berthomé, R.; Orsel, M.; Mercey-Boutet, S.; Yu, A.; Castaings, L.; Elftieh, S.; Major, H.; Renou, J.-P.; Daniel-Vedele, F. Arabidopsis roots and shoots show distinct temporal adaptation patterns toward nitrogen starvation. *Plant Physiol.* **2011**, *157*, 1255–1282. [[CrossRef](#)]
25. Luo, J.; Zhou, J.; Li, H.; Shi, W.; Polle, A.; Lu, M.; Sun, X.; Luo, Z.-B. Global poplar root and leaf transcriptomes reveal links between growth and stress responses under nitrogen starvation and excess. *Tree Physiol.* **2015**, *35*, 1283–1302. [[CrossRef](#)] [[PubMed](#)]
26. Tuteja, N.; Mahajan, S. Calcium Signaling Network in Plants. *Plant Signal. Behav.* **2007**, *2*, 79–85. [[CrossRef](#)] [[PubMed](#)]
27. de Bang, T.C.; Husted, S.; Laursen, K.H.; Persson, D.P.; Schjoerring, J.K. The molecular–physiological functions of mineral macronutrients and their consequences for deficiency symptoms in plants. *New Phytol.* **2020**, *229*, 2446–2469. [[CrossRef](#)] [[PubMed](#)]
28. Yu, J.; Zhu, M.; Wang, M.; Xu, Y.; Chen, W.; Yang, G. Transcriptome analysis of calcium-induced accumulation of anthocyanins in grape skin. *Sci. Hortic.* **2020**, *260*, 108871. [[CrossRef](#)]
29. Michailidis, M.; Titeli, V.S.; Karagiannis, E.; Feidaki, K.; Ganopoulos, I.; Tanou, G.; Argiriou, A.; Molassiotis, A. Tissue-specific transcriptional analysis outlines calcium-induced core metabolic changes in sweet cherry fruit. *Plant Physiol. Biochem.* **2022**, *189*, 139–152. [[CrossRef](#)]
30. Xu, J.; Li, L.; Liu, Y.; Yu, Y.; Li, H.; Wang, X.; Pang, Y.; Cao, H.; Sun, Q. Molecular and physiological mechanisms of strigolactones-mediated drought stress in crab apple (*Malus hupehensis* Rehd.) seedlings. *Sci. Hortic.* **2023**, *311*, 111800. [[CrossRef](#)]
31. Zhang, X.-M.; Liu, L.-X.; Su, Z.-M.; Tang, J.; Shen, Z.-J.; Gao, G.-F.; Yi, Y.; Zheng, H.-L. Expression analysis of calcium-dependent protein kinases (CDPKs) superfamily genes in *Medicago lupulina* in response to high calcium, carbonate and drought. *Plant Soil* **2019**, *441*, 219–234. [[CrossRef](#)]
32. Zhang, X.-M.; Liu, L.-X.; Su, Z.-M.; Shen, Z.-J.; Gao, G.-F.; Yi, Y.; Zheng, H.-L. Transcriptome analysis of *Medicago lupulina* seedlings leaves treated by high calcium provides insights into calcium oxalate formation. *Plant Soil* **2019**, *444*, 299–314. [[CrossRef](#)]
33. Li, F.; Zhang, Q.; Tang, M.; Yi, Y. Effect of high calcium stress on expression of genes in Arabidopsis thaliana roots. *Genom. Appl. Biol.* **2021**, *40*, 1793–1800. [[CrossRef](#)]
34. Yu, W.; Yi, Y.L.; Yang, L. Effects of different available calcium and nitrogen in soil on effectiveness of disease resistance to blight of tomato. *Soil Fertil. Sci. China* **2016**, *1*, 134–140. [[CrossRef](#)]
35. Zhang, G.C.; Dai, X.L.; Xu, Y.; Ding, H.; Ci, D.W.; Qin, F.F.; Guo, F.; Zhang, Z.M. Effect of nitrogen reduction and calcium fertilizer application on photosynthetic characteristics, yield and fertilizer contribution rate in peanut. *Chin. J. Oil Crop Sci.* **2020**, *42*, 1010–1018. [[CrossRef](#)]
36. Milani, M.; Pradella, E.M.; Heintze, W.; Schafer, G.; Bender, R.J. Nitrogen and calcium fertilization on the growth and development of gerbera cultivated in pots for cut flowers. *Ornam. Hortic.* **2021**, *27*, 288–295. [[CrossRef](#)]
37. Ozyhar, T.; Marchi, M.; Facciotto, G.; Bergante, S.; Luster, J. Combined application of calcium carbonate and NPKS fertilizer improves early-stage growth of poplar in acid soils. *For. Ecol. Manag.* **2022**, *514*, 120211. [[CrossRef](#)]
38. Dong, L.; Widagdo, F.R.A.; Xie, L.; Li, F. Biomass and volume modeling along with carbon concentration variations of short-rotation poplar plantations. *Forests* **2020**, *11*, 780. [[CrossRef](#)]
39. Zeng, W.; Chen, X.; Yang, X. Developing national and regional individual tree biomass models and analyzing impact of climatic factors on biomass estimation for poplar plantations in China. *Trees* **2021**, *35*, 93–102. [[CrossRef](#)]
40. Song, L.N.; Zhu, J.J.; Zheng, X. Forestation and management scheme of *Pinus sylpholatum* var. mongolica plantation in sandy lands based on decline mechanisms. *Chin. J. Ecol.* **2017**, *36*, 3249–3256. [[CrossRef](#)]
41. Liu, Y.L.; Xin, Z.B.; Li, Z.S.; Maierdang, K. Climate effect on the radial growth of *Populus simonii* in Northwest of Hebei for last four decades. *Acta Ecol. Sin.* **2020**, *40*, 9108–9119.
42. Huebner, L. Large scale afforestation in arid and semi-arid climate: Hydrologic-ecological lessons learned and concept of modular hydrologic connectivity of vegetation. *J. Agric. Food Dev.* **2020**, *6*, 10–21. [[CrossRef](#)]

43. Jin, Z.H. *Water-Use Efficiency of Poplar Plantation in Shunyi and the Influence Law of Environmental and Biological Factors*; Beijing Forestry University: Beijing, China, 2020.
44. Junjie, Z.; Ling, W.; Yuan, L.; Chengyuan, W.; Xuegang, M. Assessing the effects of China's Three-North Shelter Forest Program over 40 years. *Sci. Total Environ.* **2023**, *857*, 159354. [[CrossRef](#)]
45. Han, S.H.; An, J.Y.; Hwang, J.; Bin Kim, S.; Park, B.B. The effects of organic manure and chemical fertilizer on the growth and nutrient concentrations of yellow poplar (*Liriodendron tulipifera* Lin.) in a nursery system. *For. Sci. Technol.* **2016**, *12*, 137–143. [[CrossRef](#)]
46. Kaur, J.; Singh, B. Role of phosphorus and potassium nutrition in enhancing yield, nutrient use efficiency and quality of wheat under variable aged poplar (*Populus deltoides* Bartr.) plantations in India. *Agrofor. Syst.* **2022**, *96*, 1065–1075. [[CrossRef](#)]
47. Luo, J.; Zhou, J.-J. Growth performance, photosynthesis, and root characteristics are associated with nitrogen use efficiency in six poplar species. *Environ. Exp. Bot.* **2019**, *164*, 40–51. [[CrossRef](#)]
48. Zhang, J.; Zhao, Y.; Xin, Y. Changes in and evaluation of surface soil quality in *Populus* × xiaohei shelterbelts in midwestern Heilongjiang province, China. *J. For. Res.* **2021**, *32*, 1221–1233. [[CrossRef](#)]
49. Weng, X.; Li, H.; Ren, C.; Zhou, Y.; Zhu, W.; Zhang, S.; Liu, L. Calcium regulates growth and nutrient absorption in poplar seedlings. *Front. Plant Sci.* **2022**, *13*, 887098. [[CrossRef](#)]
50. Kavka, M.; Majcherczyk, A.; Kües, U.; Polle, A. Phylogeny, tissue-specific expression, and activities of root-secreted purple acid phosphatases for P uptake from ATP in P starved poplar. *Plant Sci.* **2021**, *307*, 110906. [[CrossRef](#)]
51. Wang, K.; Zhang, R.; Song, L.; Yan, T.; Na, E. Comparison of C:N:P stoichiometry in the plant-litter-soil system between poplar and elm plantations in the Horqin Sandy Land, China. *Front. Plant Sci.* **2021**, *12*, 655517. [[CrossRef](#)]
52. Xie, X.M. *Soil and Plant Nutrition Experiments*; Zhejiang University Press: Hangzhou, China, 2014.
53. Chen, G.; Li, S. *Plant Physiology Experiment*; Higher Education Press: Beijing, China, 2016; p. 2.
54. Wang, F.; Sanz, A.; Brenner, M.L.; Smith, A. Sucrose synthase, starch accumulation, and tomato fruit sink strength. *Plant Physiol.* **1993**, *101*, 321–327. [[CrossRef](#)]
55. Zhao, S.J. *The Experimental Guide for Plant Physiology*, 3rd ed.; Higher Education Press: Beijing, China, 2002.
56. Xie, H.; Yu, M.; Cheng, X. Leaf non-structural carbohydrate allocation and C:N:P stoichiometry in response to light acclimation in seedlings of two subtropical shade-tolerant tree species. *Plant Physiol. Biochem.* **2018**, *124*, 146–154. [[CrossRef](#)]
57. Perveen, S.; Saeed, M.; Parveen, A.; Javed, M.T.; Zafar, S.; Iqbal, N. Modulation of growth and key physiobiochemical attributes after foliar application of zinc sulphate (ZnSO₄) on wheat (*Triticum aestivum* L.) under cadmium (Cd) stress. *Physiol. Mol. Biol. Plants* **2020**, *26*, 1787–1797. [[CrossRef](#)]
58. Hong, S.R.; Zhu, Y.Y.; Li, Z.Y.; Hu, M.Y.; Ouyang, K.H. The plantlets of *Medicago polymorpha* L. and *Medicago sativa* L. under salt stress: Transcriptome analysis and salt tolerance gene screening. *Chin. Agric. Sci. Bull.* **2023**, *39*, 111–118. [[CrossRef](#)]
59. Fan, Y.; Lv, Z.; Qin, B.; Yang, J.; Ren, K.; Liu, Q.; Jiang, F.; Zhang, W.; Ma, S.; Ma, C.; et al. Night warming at the vegetative stage improves pre-anthesis photosynthesis and plant productivity involved in grain yield of winter wheat. *Plant Physiol. Biochem.* **2022**, *186*, 19–30. [[CrossRef](#)] [[PubMed](#)]
60. Gao, Y.-F.; Rong, L.-P.; Zhao, D.-H.; Zhang, J.-Q.; Chen, J.-S. Effects of simulated acid rain on the photosynthetic physiology of *Acer ginnala* seedlings. *Can. J. For. Res.* **2021**, *51*, 18–24. [[CrossRef](#)]
61. D'andrea, E.; Scartazza, A.; Battistelli, A.; Collalti, A.; Proietti, S.; Rezaie, N.; Matteucci, G.; Moscatello, S. Unravelling resilience mechanisms in forests: Role of non-structural carbohydrates in responding to extreme weather events. *Tree Physiol.* **2021**, *41*, 1808–1818. [[CrossRef](#)]
62. Godard, P.; Urrestarazu, A.; Vissers, S.; Kontos, K.; Bontempi, G.; van Helden, J.; André, B. Effect of 21 different nitrogen sources on global gene expression in the yeast *Saccharomyces cerevisiae*. *Mol. Cell. Biol.* **2007**, *27*, 3065–3086. [[CrossRef](#)]
63. Yi, Y.; de Jong, A.; Frenzel, E.; Kuipers, O.P. Comparative transcriptomics of *Bacillus mycoides* strains in response to potato-root exudates reveals different genetic adaptation of endophytic and soil isolates. *Front. Microbiol.* **2017**, *8*, 1487. [[CrossRef](#)]
64. Liu, M.-S.; Wang, C.-K.; Quan, X.-K. Transcriptome analysis on responses of leaf photosynthesis and nitrogen metabolism of *Larix gmelinii* to environmental change. *Chin. J. Appl. Ecol.* **2022**, *33*, 957–962. [[CrossRef](#)]
65. Luo, L.; Zhang, Y.; Xu, G. How does nitrogen shape plant architecture? *J. Exp. Bot.* **2020**, *71*, 4415–4427. [[CrossRef](#)]
66. Kahsay, W.S. Effects of nitrogen and phosphorus on potatoes production in Ethiopia: A review. *Cogent Food Agric.* **2019**, *5*, 1572985. [[CrossRef](#)]
67. Tewari, R.K.; Yadav, N.; Gupta, R.; Kumar, P. Oxidative stress under macronutrient deficiency in plants. *J. Soil Sci. Plant Nutr.* **2021**, *21*, 832–859. [[CrossRef](#)]
68. Xue, Y.; Yan, W.; Gao, Y.; Zhang, H.; Jiang, L.; Qian, X.; Cui, Z.; Zhang, C.; Liu, S.; Wang, H.; et al. Interaction effects of nitrogen rates and forms combined with and without zinc supply on plant growth and nutrient uptake in maize seedlings. *Front. Plant Sci.* **2021**, *12*, 722752. [[CrossRef](#)] [[PubMed](#)]
69. Thor, K. Calcium-Nutrient and Messenger. *Front. Plant Sci.* **2019**, *10*, 440. [[CrossRef](#)] [[PubMed](#)]
70. Martins, V.; Garcia, A.; Alhinho, A.T.; Costa, P.; Lanceros-Méndez, S.; Costa, M.M.R.; Gerós, H. Vineyard calcium sprays induce changes in grape berry skin, firmness, cell wall composition and expression of cell wall-related genes. *Plant Physiol. Biochem.* **2020**, *150*, 49–55. [[CrossRef](#)] [[PubMed](#)]

71. Balantič, K.; Weiss, V.U.; Allmaier, G.; Kramar, P. Calcium ion effect on phospholipid bilayers as cell membrane analogs. *Bioelectrochemistry* **2022**, *143*, 107988. [[CrossRef](#)] [[PubMed](#)]
72. Malik, Z.; Afzal, S.; Danish, M.; Abbasi, G.H.; Bukhari, S.A.H.; Khan, M.I.; Dawood, M.; Kamran, M.; Soliman, M.H.; Rizwan, M.; et al. Role of Nitric Oxide and Calcium Signaling in Abiotic Stress Tolerance in Plants. In *Protective Chemical Agents in the Amelioration of Plant Abiotic Stress*; Wiley: Hoboken, NJ, USA, 2020; pp. 563–581. [[CrossRef](#)]
73. Parvin, K.; Nahar, K.; Hasanuzzaman, M.; Bhuyan, M.H.M.B.; Fujita, M. Calcium-Mediated Growth Regulation and Abiotic Stress Tolerance in Plants. In *Plant Abiotic Stress Tolerance*; Springer: Cham, Switzerland, 2019; pp. 291–331. [[CrossRef](#)]
74. Wang, Y.; Shen, C.; Jiang, Q.; Wang, Z.; Gao, C.; Wang, W. Seed priming with calcium chloride enhances stress tolerance in rice seedlings. *Plant Sci.* **2022**, *323*, 111381. [[CrossRef](#)]
75. Tuna, A.L.; Kaya, C.; Ashraf, M.; Altunlu, H.; Yokas, I.; Yagmur, B. The effects of calcium sulphate on growth, membrane stability and nutrient uptake of tomato plants grown under salt stress. *Environ. Exp. Bot.* **2007**, *59*, 173–178. [[CrossRef](#)]
76. Dimkpa, C.O.; Fugice, J.; Singh, U.; Lewis, T.D. Development of fertilizers for enhanced nitrogen use efficiency—Trends and perspectives. *Sci. Total Environ.* **2020**, *731*, 139113. [[CrossRef](#)]
77. Fenn, L.B.; Taylor, R.M.; Binzel, M.L.; Burks, C.M. Calcium stimulation of ammonium absorption in onion. *Agron. J.* **1991**, *83*, 840–843. [[CrossRef](#)]
78. Fu, L.L. *The Effect of Exogenous Calcium on Nitrogen Absorption and Utilization of Apple*; Shandong Agricultural University: Tai'an, China, 2020.
79. Zou, W.T.; Huang, Z.S.; Wang, C.W. Effects of different amounts of nitrogen and calcium on agronomic characters and dry weight of flue-cured tobacco. *Guangdong Agric. Sci.* **2016**, *43*, 25–30. [[CrossRef](#)]
80. Van Assche, F.; Clijsters, H. Effects of metals on enzyme activity in plants. *Plant Cell Environ.* **1990**, *13*, 195–206. [[CrossRef](#)]
81. Yin, L.; Hu, T.X.; Liu, Y.A.; Xie, C.Y.; Feng, Y.; Yan, Z.; Li, Y.H.; Wang, Y.J. Effect of nitrogen application rate on growth and leaf photosynthetic characteristics of *Jatropha curcas* L. seedlings. *Acta Ecol. Sin.* **2011**, *31*, 4977–4984.
82. Li, Z.Y.; Zhang, Y.; Han, L.H.; Xu, J.Z. The interactive effects of nitrogen and calcium on photosynthetic characteristics and chlorophyll fluorescence parameters of nectarine under protected culture. *J. Plant Nutr. Fertil. Ers* **2013**, *19*, 893–900. [[CrossRef](#)]
83. Yu, D.; Gu, X.; Zhang, S.; Dong, S.; Miao, H.; Gebretsadik, K.; Bo, K. Molecular basis of heterosis and related breeding strategies reveal its importance in vegetable breeding. *Hortic. Res.* **2021**, *8*, 1–17. [[CrossRef](#)] [[PubMed](#)]
84. Wang, Y.; Wu, W.-H. Regulation of potassium transport and signaling in plants. *Curr. Opin. Plant Biol.* **2017**, *39*, 123–128. [[CrossRef](#)]
85. Hajihashemi, S.; Skalicky, M.; Brestic, M.; Pavla, V. Cross-talk between nitric oxide, hydrogen peroxide and calcium in salt-stressed *Chenopodium quinoa* Willd. At seed germination stage. *Plant Physiol. Biochem.* **2020**, *154*, 657–664. [[CrossRef](#)]
86. Yang, S.; Wang, J.; Tang, Z.; Guo, F.; Zhang, Y.; Zhang, J.; Meng, J.; Zheng, L.; Wan, S.; Li, X. Transcriptome of peanut kernel and shell reveals the mechanism of calcium on peanut pod development. *Sci. Rep.* **2020**, *10*, 15723. [[CrossRef](#)]
87. Liu, Y.; Wang, H.; Jiang, Z.; Wang, W.; Xu, R.; Wang, Q.; Zhang, Z.; Li, A.; Liang, Y.; Ou, S.; et al. Genomic basis of geographical adaptation to soil nitrogen in rice. *Nature* **2021**, *590*, 600–605. [[CrossRef](#)]
88. Sun, T.; Zhang, J.; Zhang, Q.; Li, X.; Li, M.; Yang, Y.; Zhou, J.; Wei, Q.; Zhou, B. Transcriptome and metabolome analyses revealed the response mechanism of apple to different phosphorus stresses. *Plant Physiol. Biochem.* **2021**, *167*, 639–650. [[CrossRef](#)]
89. Xu, Y.; Li, X.; Lin, J.; Wang, Z.; Yang, Q.; Chang, Y. Transcriptome sequencing and analysis of major genes involved in calcium signaling pathways in pear plants (*Pyrus calleryana* Decne.). *BMC Genom.* **2015**, *16*, 738. [[CrossRef](#)]
90. Sun, T.; Zhang, J.; Zhang, Q.; Li, X.; Li, M.; Yang, Y.; Zhou, J.; Wei, Q.; Zhou, B. Integrative physiological, transcriptome, and metabolome analysis reveals the effects of nitrogen sufficiency and deficiency conditions in apple leaves and roots. *Environ. Exp. Bot.* **2021**, *192*, 104633. [[CrossRef](#)]
91. Shi, Y.J.; Liu, D.; He, Y.Q.; Li, Q.R.; Luo, J.S.; Zhang, Z.H. Physiological and molecular mechanisms of Arabidopsis thaliana wild-type Col-0 responds to low nitrogen. *Plant Physiol. J.* **2022**, *58*, 1779–1789. [[CrossRef](#)]
92. Pathak, J.; Ahmed, H.; Kumari, N.; Pandey, A.; Rajneesh; Sinha, R.P. Role of calcium and potassium in amelioration of environmental stress in plants. In *Protective Chemical Agents in the Amelioration of Plant Abiotic Stress: Biochemical and Molecular Perspectives*; John Wiley & Sons Ltd.: Hoboken, NJ, USA, 2020; pp. 535–562. [[CrossRef](#)]
93. Ligaba-Osena, A.; Salehin, M.; Numan, M.; Wang, X.; Choi, S.-C.; Jima, D.; Bobay, L.-M.; Guo, W. Genome-wide transcriptome analysis of the orphan crop tef (*Eragrostis tef* (Zucc.) Trotter) under long-term low calcium stress. *Sci. Rep.* **2022**, *12*, 19552. [[CrossRef](#)] [[PubMed](#)]
94. Liu, Q.; Li, Y.; Liao, G.; Xu, X.; Jia, D.; Zhong, M.; Wang, H.; Ye, B. Transcriptome and Metabolome reveal AsA regulatory network between metabolites and genes after fruit shading by bagging in kiwifruit (*Actinidia eriantha*). *Sci. Hort.* **2022**, *302*, 111184. [[CrossRef](#)]
95. Xu, Z.; Dong, M.; Peng, X.; Ku, W.; Zhao, Y.; Yang, G. New insight into the molecular basis of cadmium stress responses of wild paper mulberry plant by transcriptome analysis. *Ecotoxicol. Environ. Saf.* **2019**, *171*, 301–312. [[CrossRef](#)]
96. Pinto, E.; Fidalgo, F.; Teixeira, J.; Aguiar, A.A.; Ferreira, I.M. Influence of the temporal and spatial variation of nitrate reductase, glutamine synthetase and soil composition in the N species content in lettuce (*Lactuca sativa*). *Plant Sci.* **2014**, *219*, 35–41. [[CrossRef](#)]
97. Liu, X.; Zhao, J.; Nan, F.; Liu, Q.; Lv, J.; Feng, J.; Xie, S. Transcriptome Analysis Reveals the Mechanisms of Tolerance to High Concentrations of Calcium Chloride Stress in *Parachlorella kessleri*. *Int. J. Mol. Sci.* **2023**, *24*, 651. [[CrossRef](#)]

98. Liu, X.; Yin, C.; Xiang, L.; Jiang, W.; Xu, S.; Mao, Z. Transcription strategies related to photosynthesis and nitrogen metabolism of wheat in response to nitrogen deficiency. *BMC Plant Biol.* **2020**, *20*, 448. [[CrossRef](#)]
99. Li, Y.; Wang, M.; Teng, K.; Dong, D.; Liu, Z.; Zhang, T.; Han, L. Transcriptome profiling revealed candidate genes, pathways and transcription factors related to nitrogen utilization and excessive nitrogen stress in perennial ryegrass. *Sci. Rep.* **2022**, *12*, 3353. [[CrossRef](#)]

Disclaimer/Publisher's Note: The statements, opinions and data contained in all publications are solely those of the individual author(s) and contributor(s) and not of MDPI and/or the editor(s). MDPI and/or the editor(s) disclaim responsibility for any injury to people or property resulting from any ideas, methods, instructions or products referred to in the content.